[1] Ankur Agarwal*

Fusion of Remote Sensing Images using Signal Decomposition Methods: A Comparative Analysis

Journal of Electrical Systems

Abstract: - An efficient method for extending the depth-of-field of optical lenses is multi-focus image fusion, which produces an entirely focused image from a collection of partly focused images of the same scheme. In this paper, fusion schemes namely, Self Fractional Fourier Functions, 2D- Variational mode decomposition, 2D- Variational mode decomposition with fusion rule, Bidimensional multivariate Empirical mode Decomposition, and 2D-Compact Variational mode decomposition are compared for Remote sensing images for fusion. Also, a novel approach is derived and compared with the above-stated algorithms. The simulations are performed on available data sets and compared with the existing algorithms using seventeen objective performance parameters and subjective parameters. The simulation results show that the proposed algorithm gives better results than the existing schemes.

Keywords: Image fusion, 2-dimensional Variational mode decomposition, Bidimensional multivariate Empirical mode Decomposition, 2-dimensional Compact Variational mode decomposition, Self Fractional Fourier Functions.

1. Main text

Data fusion can be defined as the synergistic use of information from different sources to assist in the overall understanding of a phenomenon. For the last 19 years (from 2005 to 2023) data is acquired from the Core Collection database of Web of Science (WoS) and presented in Figure 1. Which witnesses the development in this field with an increase in newly proposed methods. [5,6].

Multi-focus image fusion works well to increase the depth of field of optical lenses by creating an all-in-focus image from a collection of partially focused images. This technique is important in the domains of digital photography, integral imaging, optical microscopy, etc. Image Fusion techniques can be classified as frequency and spatial domain.

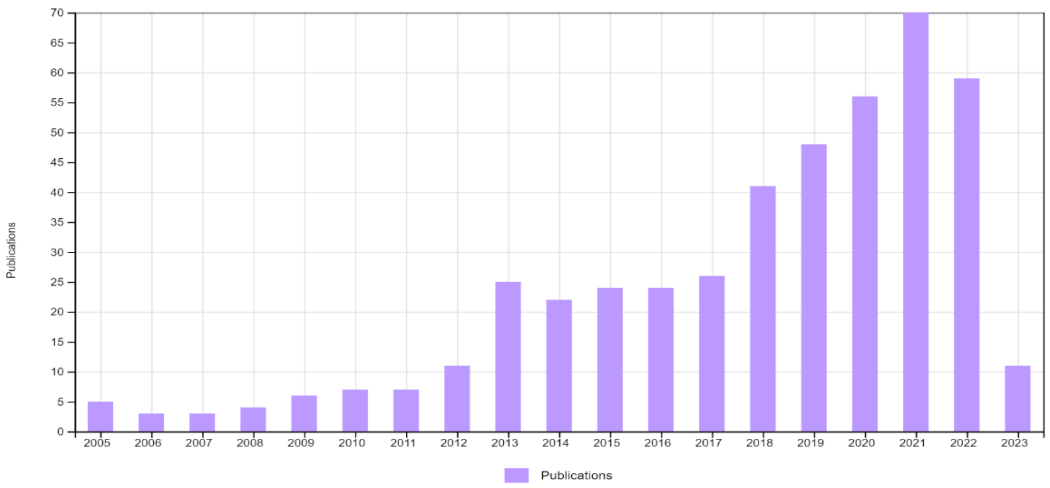

Fig. 1 Articles available in international journals indexed by Science Citation Index Expanded (SCIE) of duration from 2005 to 2023, on multi-focus image fusion are shown here.

A fully data-driven technique namely EMD, which decomposes signals into their basic components, called intrinsic mode functions (IMFs) [12,16,21], which is a different approach from the Fourier transform or wavelet transform-based signal decomposition methods that project signals onto a fixed set of bases. Empirical Mode decomposition (EMD)[4] and its variants like multivariate EMD (MEMD)[10], Bivariate EMD, Multivariate EMD, Multidimensional Empirical mode decomposition, Bidimensional Multivariate Empirical Mode decomposition, Window EMD, methods for multi-focus image fusion have recently been reported. Thereafter VMD [2,3] came into existence as a robust tool for processing the non-stationary signal. It has been suggested in the literature that, the VMD performance is superior to EMD and its modified forms in terms of noise robustness, tone detection, and tone separation [2,3], and also has an appropriate mathematical theory. The image fusion classification techniques, categorization, and applications are summarised in Figure 2.[8,9,11,26]

[1]* Department of Electronics and Communication Engineering, Malviya National Institute of Technology, Jaipur and 302017, India

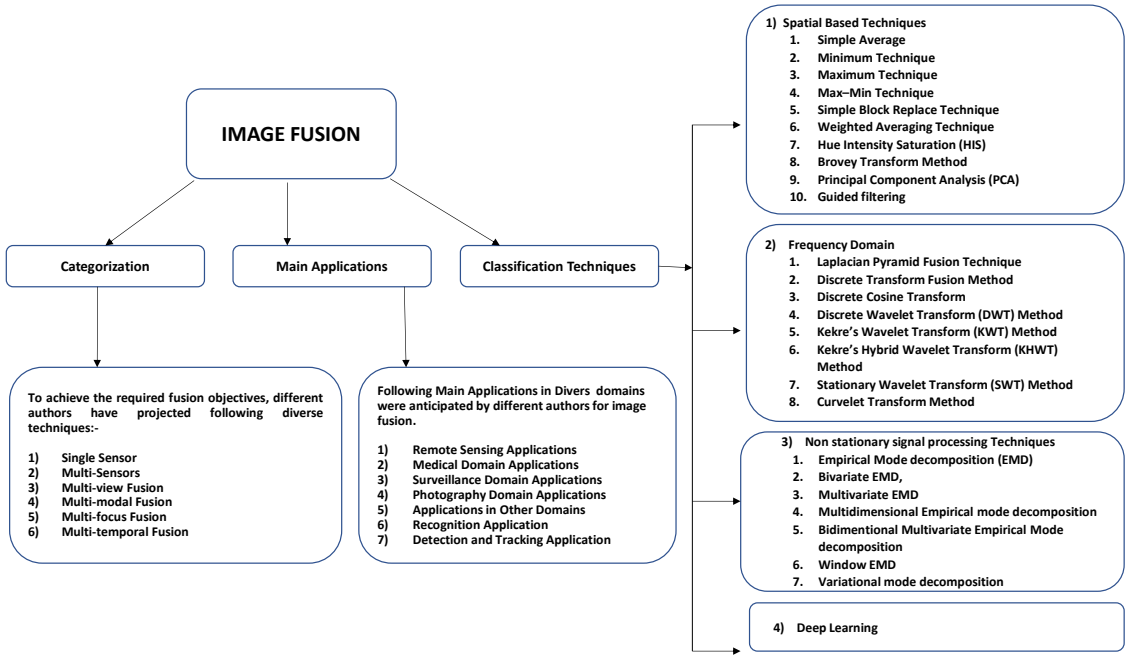

Fig.2. Classification of Image Fusion techniques

2. Literature review

2.1. Self-Factional Fourier Functions (SFFF)

Self-fractional Fourier functions $\psi(t)_{M,L}$, which are Eigen functions of the fractional Fourier operation, are invariant under the fractional Fourier transform for some angle α. Any function let $\varphi(t)$, from The Hilbert space of finite space i.e. L^2, can be represented as a sum of M SFFF which are orthogonal to each other. Let $\varphi(x,y)$ be any generator function, which can be represented through the sum of M orthogonal SFFFs of the order M

$$\varphi(x,y) = \sum_{L=0}^{M} \psi(x,y)_{M,L} \tag{1}$$

Where

$$\psi(x,y)_{M,L} = \frac{1}{M}\sum_{k=1}^{M} \exp\left(\frac{i2\pi L(k-1)}{M}\right) R^{(\alpha,\alpha)}[\varphi(u,v)](x,y) \tag{2}$$

Here $\psi(x,y)_{M,L}$ is an SFFF's, $R^{(\alpha,\alpha)}$denotes a 2D-FRFT operator with angle $\alpha = \frac{2\pi(k-1)}{M}$ towards the axis x, and y.[23]

2.2. Bidimensional MEMD Algorithm

The bidimensional MEMD algorithm for ready reference is given below [1]. The bidimensional multivariate signal S can be decomposed into K bidimensional univariate signals, represented as Q^{φ_k}, for k = 1,2,…,K, by projecting S along v^{φ_k}. The algorithm is stated below

Algorithm1: Bidimensional MEMD Algorithm

1. Evaluate the projections of bidimensional multivariate signal S along the unit projection vector v^{φ_k} by the following equation (3), and denoted by Q^{φ_k}

$$Q^{\varphi_k} = \begin{bmatrix} \sum_{l=1}^{n} v_l^{\varphi_k} S_l(1,1) & \sum_{l=1}^{n} v_l^{\varphi_k} S_l(1,2) & \cdots \\ \sum_{l=1}^{n} v_l^{\varphi_k} S_l(2,1) & \sum_{l=1}^{n} v_l^{\varphi_k} S_l(2,2) & \cdots \\ \vdots & \vdots & \ddots \end{bmatrix} \tag{3}$$

Where v^{φ_k} given a unit projection vector along the angle φ_k.

2. Corresponding to the local maximum and minimum of, locations $\left(x_{max}^{\varphi_k}, y_{max}^{\varphi_k}\right)$ and $\left(x_{min}^{\varphi_k}, y_{min}^{\varphi_k}\right)$ are extracted, respectively.

3. n-dimensional maximal and minimal surfaces are obtained by interpolation of $S\left(x_{max}^{\varphi_k}, y_{max}^{\varphi_k}\right)$ and $S\left(x_{min}^{\varphi_k}, y_{min}^{\varphi_k}\right)$ represented by $\varepsilon_{max}^{\varphi_k}$ and $\varepsilon_{min}^{\varphi_k}$ respectively.

4. Repeat the above steps for all k from 1 to K.

5. μ which is the n-dimension mean surface of S is estimated as,

$$\mu = \frac{1}{2K}\sum_{k=1}^{K}\left(\varepsilon_{max}^{\varphi_k} + \varepsilon_{min}^{\varphi_k}\right). \tag{4}$$

6. Extract the details β using $\beta = S - \mu$.

If β satisfies the 2D stopping condition [24].[25]. For a bidimensional n-variate IMF, apply the above procedure to $S - \beta$, otherwise apply it to β.

2.3. Variational Mode Decomposition

The time-frequency signal analysis method VMD is completely adaptive and non-recursive. An original time series x is divided into n IMFs using the VMD. Dragomirestskiy and Zossa [3] claim that equation (1) is the constrained variational formulation for generating the IMFs.

$$\min_{\{u_n\},\ \{\omega_n\}} \left\{ \sum_{n=1}^{N} \left\| \partial t \left[\left(\delta(t) + \frac{j}{\pi t} \right) * u_n(t) \right] e^{-j\omega_n t} \right\|_2^2 \right\}, \qquad s.t. \sum_{n=1}^{N} u_n(t) = x(t) \tag{5}$$

Where δ = the Delta function; j^2 = -1; $\|.\|_2$ = L_2 distance; ω_n = the center frequency; * = the convolution; $u_n(t) = A_n \cos(\emptyset_n(t))$ the n^{th} IMF; $\emptyset_n$ = the non-decreasing function; and A_n = the non-negative function.[2,3].

2.4. 2D Compact Variational Mode Decomposition

For the amplitude discontinuities or abrupt changes, the performance of 1D-VMD suffers. To overcome this drawback of intrinsic conflict, as there is an inverse relationship between frequency and spatial support, Zassol et. Introduced 2D-CVMD an extension of VMD [34]. The binary support function is introduced in 2D-CVMD to eliminate abrupt signal conditions. The generalization of the Hilbert transform, directional Hilbert transform to higher dimensions is used in 2D-CVMD. To promote the sparsity of the signal L1-norm penalty function and total-variance (TV) are used. Finally, ADMM is used to solve the optimization problem, as ADMM is multiple times faster than conventional methods. Iteratively by ADMM, the modes Center frequencies, and Lagrangian multiplier are updated until the convergence criteria are satisfied [34].

2.5. Objective performance parameters are used for the comparison of the proposed algorithm with the others.

Due to the nonavailability of ground truth images in some applications as in this application, performance evaluation becomes a tedious task. Various performance parameters have been proposed by researchers for this issue [4,7,18,33,36,37]. The following sixteen parameters including simulation time, were used in this paper for the comparison of the performance of different algorithms.

1. Information Theory-Based Metrics
1. Normalized Mutual Information (P_{MI})[14]
2. Image Feature-Based Metrics
1. Nonlinear Correlation Information Entropy (P_{NCIE})
2. Gradient-Based Fusion Performance (P_G)
3. Image Fusion Metric-Based on Phase Congruency (P_P)
3. Image Structural Similarity-Based Metrics
1. Piella's Metric (P_S)[28]
2. Yang's Metric (P_Y)
4. Human Perception Inspired Fusion Metrics
1. Chen-Blum Metric (P_{CB})[23,29]
2. Chen-Varshney Metric (P_{CV})[30]

For all eight parameters from serial No. 1 to 4, except for (P_{CV}), a higher value shows better fusion performance, whereas a lower value shows better fusion performance for (P_{CV}) is just on the contrary.[7].

5. Mean or Average Pixel Intensity (Mean): Measure of contrast.
6. Standard Deviation (SD): Measure of the spread of data.
7. Average Gradient (AG): Measure of degree of clarity and sharpness.
8. Spatial Frequency (SF): Measure of activity level in the region.
9. Total fusion performance ($Q^{AB/F}$): Measure of total information transfer from source image to fused image.
10. Fusion loss ($L^{AB/F}$): Total loss of information.
11. Fusion artifacts ($N^{AB/F1}$): Noise or artifacts added in the fusion process.
12. Fusion artifact modified ($N^{AB/F}$): Noise or artifacts added in fusion process modified parameter.

For all eight parameters from serial No. 6 to 13, except for ($L^{AB/F}$), $N^{AB/F}$, a higher value shows better fusion performance, whereas a lower value shows better fusion performance for ($L^{AB/F}$, $N^{AB/F1}$, $N^{AB/F}$) is just on the contrary. [33,36,37]. Simulations are performed on Processor Intel(R) Core(TM) i7-8650U CPU@1.90GHz 2.11 GHz, RAM 16.0 GB (15.8 GB usable), System type-64-bit operating system, x64-based processor

2.6. Dataset

The dataset is taken from the link given in the book by G. Xiao, D. P. Bavirisetti, G. Liu, and X. Zhang, Titled "Image Fusion". Publisher Springer,2020 [35]. The datasethas a set of 42 images for remote sensing, out of these 42 sets simulation is performed on three sets of images.

3. A Novel approach (Proposed)

3.1 The Proposed Fusion Algorithm for grayscale image

1. Read the bidimensional multiscale images $S(x, y)$
2. Calculate 2-D IMFs of the images $S(x, y)'s$ using 2D- Compact Variational Mode Decomposition.
3. Calculate the new IMFs by concatenating the corresponding IMFs from the images.
4. Repeat for all M, IMF to find a set of fused IMFs, for m=1, 2…. M.
5. Add all $\bar{S}^m(x, y)$to gather to yield the fused image $\bar{S}(x, y)$.

3. Methodology for novel approach

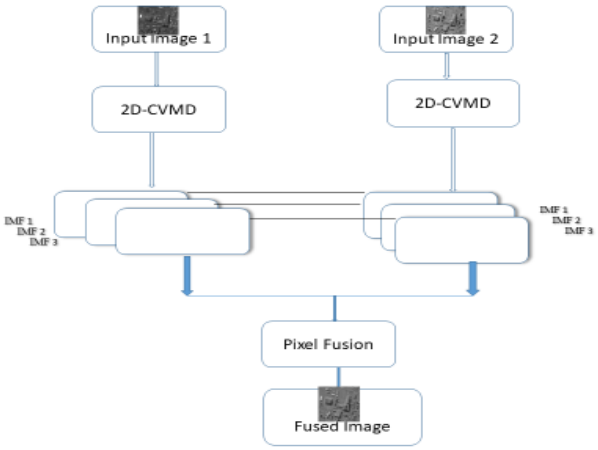

Fig. 3 Structure of the proposed algorithm for gray-scale image.

3.3 Formulation of Novel Approach

The methodology of the 2-D CVMD-based multi-scale image fusion at the pixel level is explained in Figure 3. A bidimensional multivariate signal $S(x,y)$, which is a collection of n images (two images in this case) as illustrated in equation 6 for grayscale images, is first disintegrated by the 2-D CVMD method to find a set of M, n-variate IMF images denoted by $S_k^m(x,y)$ where m=1, 2 ….M and k=1,2,……n. as

For graysscale images

$$\left\{S(x,y): \left|S_k^m(x,y) \quad \begin{matrix} m = 1,2,\ldots.MDenotes\ IMF's \\ k = 1,2,\ldots.nDenotesde-focused\ \text{images} \end{matrix}\right|\right\} \tag{6}$$

$$\text{where} \left\{ S_k^m(x,y): \left| \begin{matrix} S_1^m(x,y) = \sum_{m=1}^{M} S_1^m(x,y) \text{ where } \begin{vmatrix} S_1^1(x,y) & \text{1st IMF of first image} \\ \vdots & \vdots \\ S_1^m(x,y) & \text{Mth IMF of first image} \end{vmatrix} \\ \vdots \\ S_n^m(x,y) = \sum_{m=1}^{M} S_n^m(x,y) \text{ where } \begin{vmatrix} S_n^1(x,y) & \text{1st IMF of nth image} \\ \vdots & \vdots \\ S_n^m(x,y) & \text{Mth IMF of nth image} \end{vmatrix} \end{matrix} \right| \right\}$$

Here symbol |⬚| in the equation (6) is used to define the signal that does not represent an operator, In the next step, Calculate the resultant IMFs by adding the respective IMFs from the input images as given in equation (7).

$$I_k^m(x,y) = \sum_{m=1}^{M} S_k^m(x,y) \qquad \text{for k = 1 to n.} \tag{7}$$

To calculate all m IMFs, to find a set of fused IMFs$\bar{S}^m(x,y)$, for m=1,2,….M, the process is repeated, finally added together to produce the fused image $\bar{S}(x,y)$.

$$\bar{S}(x,y) = \sum_{k=1}^{n} I_k^m(x,y) \tag{8}$$

4. Results

4.1 Comparison of different algorithms is made on Performance Parameters for three sets of images.

Table 1 Objective performance parameters for the first set of greyscale images of size 512x512, shown in Figure 4.

Methods / Parameters	2D-CVMD	2D-VMD with Fusion rule	2D-VMD	BMEMD with Fusion rule	SFFF
P_{MI}	**0.3340**	0.3058	0.3279	0.2873	0.1729
P_{NCIE}	**0.8043**	0.8041	0.8042	0.8039	0.8023
P_G	**0.4867**	0.4661	0.4630	0.4733	0.0324
P_P	**0.4033**	0.3538	0.3827	0.3113	0.1844
P_S	0.4749	0.5589	0.4591	**0.5856**	0.0234
P_Y	0.6896	0.7079	0.6539	**0.7223**	0.0450
P_{CB}	**0.5466**	0.4675	0.5420	0.5422	0.2295
P_{CV}	180.2330	**180.1216**	593.1186	444.2635	$1.181x10^3$
Q_F^{AB}	**0.8114**	0.7916	0.7997	0.8060	0.5611
L_F^{AB}	0.0983	0.1802	**0.0916**	0.1568	0.1927
N_{F1}^{AB}	0.4186	**0.1151**	0.4853	0.1580	0.4923
N_F^{AB}	**0.093**	0.0282	0.1087	0.0373	0.2461
Mean	**208.6157**	110.2654	208.7104	109.6497	0.8185

SD	**44.7578**	26.5399	45.1860	28.6093	0.1783
AG	10.8402	12.0829	**14.1052**	11.8470	0.0522
SF	16.9176	**17.6924**	21.0054	17.4018	NC
Simulation Time	**48.3577 Sec**	656.3904 Sec	647.5420 Sec	6483.2874 Sec	24.6188 Sec

(a) Input-1

(b) Input-2

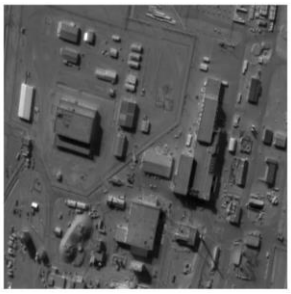

(c) SFFF

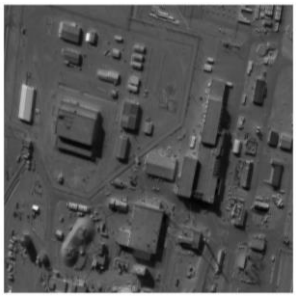

(d) 2D-VMD

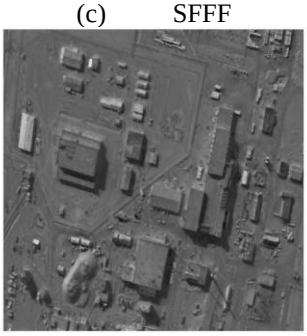

(e) BMEMD

(f) 2D-VMD Variance

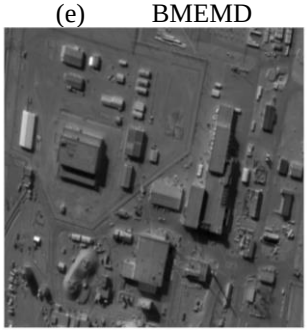

(g) 2D-CVMD

Figure.4 Images (a), and (b) are the input images for table 1, respectively, images(c), (d), (e), (f), (g) are the focused Images by SFFF only, VMD only, BMEMD, 2D-VMD with Varience and 2D-CVMD method respectively.

Table 2 Objective performance parameters for the second set of greyscale images of size 512x512, shown in figure 5

Methods / Parameters	**2D-CVMD**	**2D-VMD with Fusion rule**	**2D-VMD**	**BMEMD with Fusion rule**	**SFFF**
$\mathbf{P_{MI}}$	**0.3792**	0.3560	0.3821	0.3458	0.2099
$\mathbf{P_{NCIE}}$	**0.8056**	0.8056	0.8056	0.8054	0.8025
$\mathbf{P_G}$	**0.5126**	0.4896	0.5061	0.4837	0.0439
$\mathbf{P_P}$	**0.4135**	0.3524	0.4193	0.2955	0.2425
$\mathbf{P_S}$	0.5213	**0.5664**	0.5143	0.5615	0.0411

$\mathbf{P_Y}$	**0.7233**	0.6670	0.7075	0.7081	0.0507
$\mathbf{P_{CB}}$	0.5443	0.5187	0.5096	**0.5615**	0.2256
$\mathbf{P_{CV}}$	418.0736	382.7809	694.4588	**355.5832**	$1.127x10^3$
$\mathbf{Q_F^{AB}}$	**0.8126**	0.8090	0.8055	0.8082	0.5605
$\mathbf{L_F^{AB}}$	0.1015	0.1531	**0.0854**	0.1493	0.1963
$\mathbf{N_{F1}^{AB}}$	0.4128	**0.1471**	0.5354	0.1809	0.4864
$\mathbf{N_F^{AB}}$	0.0859	**0.0378**	0.1090	0.0425	0.2432
Mean	**202.1876**	114.4511	202.2741	114.0672	0.7932
SD	**89.7692**	35.5088	60.2625	38.4656	0.2360
AG	10.2146	**13.1402**	12.0835	11.3895	0.0484
SF	15.6733	**18.3848**	18.1641	16.1274	NC
Simulation Time	**48.0736 Sec**	778.58 Sec	738.444 Sec	4664.6046 Sec	44.5724 Sec

(a) Input-1

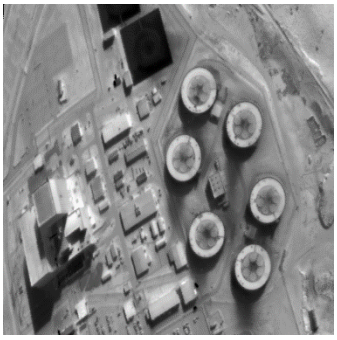

(b) Input-2

(c) SFFF

(d) 2D-VMD

(e) BMEMD

(f) 2D-VMD Variance

(g) 2D-CVMD

Figure.5 Images (a), (b) are the input images for Table 2, respectively, images(c), (d), (e), (f), and (g) are the focused Images by SFFF only, VMD only, BMEMD, 2D-VMD with Varience and 2D-CVMD method respectively.

Table 3 Objective performance parameters for the third set of greyscale images of size 512x512, shown in Figure 6.

Methods / Parameters	2D-CVMD	2D-VMD with Fusion rule	2D-VMD	BMEMD with Fusion rule	SFFF
$\mathbf{P_{MI}}$	**0.3787**	0.3381	0.3644	0.3103	0.2278
$\mathbf{P_{NCIE}}$	**0.8063**	0.8055	0.8059	0.8051	0.8029
$\mathbf{P_G}$	0.5001	**0.5095**	0.4387	0.5141	0.0795
$\mathbf{P_P}$	0.4316	**0.4405**	0.4115	0.3778	0.1094
$\mathbf{P_S}$	0.4474	0.5808	0.4118	**0.5935**	0.0768
$\mathbf{P_Y}$	0.6882	**0. 7793**	0.6488	0.7602	0.1441
$\mathbf{P_{CB}}$	**0.5409**	0.5127	0.5004	0.5535	0.3441
$\mathbf{P_{CV}}$	**418.4523**	424.8637	$1.055x10^3$	827.1156	$1.1899x10^3$
$\mathbf{Q_F^{AB}}$	0.7979	0.8252	0.7572	**0.82751**	0.5676
$\mathbf{L_F^{AB}}$	0.0989	0.1325	**0.0831**	0.1405	0.1745
$\mathbf{N_{F1}^{AB}}$	0.4320	0.1867	0.6099	**0.1397**	0.5158
$\mathbf{N_F^{AB}}$	0.1032	0.0423	0.1597	**0.0320**	0.2579
Mean	**263.5241**	141.2496	263.440	140.3213	1.0331
SD	100.1464	58.4270	**102.1248**	73.0762	0.3981
AG	23.3373	25.881	32.8001	**26.2123**	0.1129
SF	33.8724	35.5656	47.6950	**90.6504**	NC
Simulation Time	**48.7054 Sec**	977.7455 Sec	655.8218 Sec	6597.052 Sec	22.6399 Sec

(a) Input-1

(b) Input-2

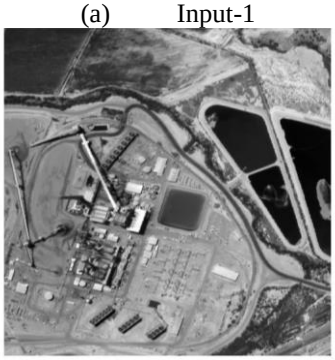

(c) SFFF

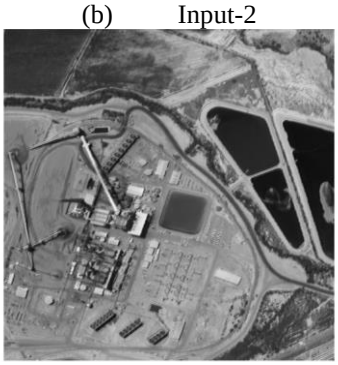

(d) 2D-VMD

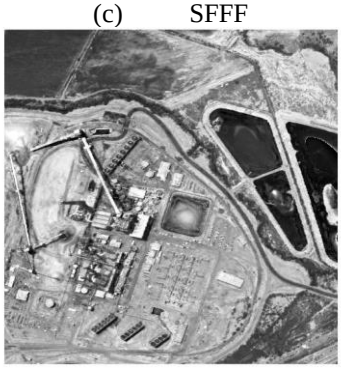

(e) BMEMD

(f) 2D-VMD Variance

(g) 2D-CVMD

Figure.6 Images (a), (b) are the input images for table 3, respectively, images(c), (d), (e), (f), and (g) are the focused Images by SFFF only, VMD only, BMEMD, 2D-VMD with Varience and 2D-CVMD method respectively.

5. Conclusion and future work

The performance is measured using the seventeen objective performance parameters, on the three grayscale images set of size 512x512 out of 42 images set available.

Experiment results show better visual perception from the fused images for 2D-CVMD, 2D-VMD with variance, 2D-VMD, and BMEMD and best for 2D-CVMD. Objective parameters like (P_{MI}, P_{NCIE}, P_G, P_P, P_{CB}, Q_F^{AB}, Mean Standard Deviation and simulation time) shows the better performance of the 2D-CVMD algorithm, whereasparameters (P_Y) show the better performance of 2D-VMD, and parameters (P_S, AG, SF) show the better performance of the BMEMD algorithm. Considering the simulation time 2D-CVMD presents the second least time with SFFF, but with comparable difference only. Concluding 2D-VMD performance is better than SFFF and BMEMD, and 2D-CVMD showed better performance comparing the above all.

Further parametric (for example variance, minima, maxima, Local energy maxima , or any other), formulation may be derived for the number of modes for decomposition of image using 2D-VMD or 2D-VMD with variance or 2D-CVMD for optimal results. Further with 2D-CVMD any other information extraction method (for example variance, minima, maxima, local energy maxima, or any other) may be used for better fusion performance. Experiments may be conducted for specific images in Remote sensing.

REFERENCES

[1] Dogra, B. Goyal, and S. Agrawal, "From multi-scale decomposition tonon-multi-scale decomposition methods: a comprehensive survey of imagefusion techniques and its applications," IEEE Access, vol. 5, pp. 16040–16067,2017.

[2] K. Dragomiretskiy and D. Zosso, "Variational mode decomposition," IEEEtransactions on signalprocessing,vol.62,no.3,pp.531–544,2013.

[3] K. Dragomiretskiy, Variational methods in signal decomposition and imageprocessing.PhDthesis,UCLA,2015.

[4] N. E. Huang, Z. Shen, S. R. Long, M. C. Wu, H. H. Shih, Q. Zheng, N.-C.Yen, C. C. Tung, and H. H. Liu, "The empirical mode decomposition andthe hilbert spectrum for nonlinear and non-stationary time series analy-sis," Proceedings of the Royal Society of London. Series A: mathematical,physicalandengineeringsciences,vol.454,no.1971,pp.903–995,1998.

[5] H.Kaur,D.Koundal,andV.Kadyan,"Imagefusiontechniques:asurvey,"Archives of computational methods in Engineering, vol. 28, pp. 4425–4447,2021.

[6] S. Li, X. Kang, L. Fang, J. Hu, and H. Yin, "Pixel-level image fusion: Asurvey of the state of the art," information Fusion, vol. 33, pp. 100–112,2017.

[7] Z. Liu, E. Blasch, Z. Xue, J. Zhao, R. Laganiere, and W. Wu, "Objectiveassessmentofmultiresolutionimagefusionalgorithmsforcontextenhance-ment in night vision: a comparative study," IEEE transactions on patternanalysisandmachineintelligence, vol. 34,no. 1, pp. 94–109, 2011.

[8] Y.Liu,L.Wang,J.Cheng,C.Li,andX.Chen,"Multi-focusimagefusion:A survey of the state of the art," Information Fusion, vol. 64, pp. 71–91,2020.

[9] D. Looney and D. P. Mandic, "Multiscale image fusion using complex ex-tensions of emd," IEEE Transactions on Signal Processing, vol. 57, no. 4,pp.1626–1630,2009.

[10] D. Mendlovic, H. M. Ozaktas, and A. W. Lohmann, "Self fourier functionsand fractional fourier transforms," Optics communications, vol. 105, no. 1-2,pp.36–38,1994.

[11] Morris and R. Rajesh, "Survey of spatial domain image fusion tech-niques," Int JAdv Res Comput Sci Eng Inf Technol, vol. 2, no. 3, pp. 249–254,2014.

[12] N. u. Rehman, D. Looney, T. Rutkowski, and D. Mandic, "Bivariate emd-basedimagefusion,"in2009IEEE/SP15thWorkshoponStatisticalSignalProcessing,pp.57–60,IEEE,2009.

[13] J. B. Sharma, K. Sharma, and V. Sahula, “Hybrid image fusion schemeusing self-fractional fourier functions and multivariate empirical mode de-composition,”SignalProcessing,vol.100,pp.146–159,2014.
[14] K. Sharma and M. Sharma, “Image fusion based on image decompositionusing self-fractional fourier functions,” Signal, image and video processing,vol.8,pp.1335–1344,2014.
[15] M. Sharma, “A review: image fusion techniques and applications,” Int JComputSciInfTechnol,vol.7,no.3,pp.1082–1085,2016.
[16] T.Stathaki,Imagefusion:algorithmsandapplications.Elsevier,2011.
[17] N. ur Rehman and H. Aftab, “Multivariate variational mode decomposi-tion,” IEEE Transactions on signal processing, vol. 67, no. 23, pp. 6039–6052,2019.
[18] Z. Wang, A. C. Bovik, H. R. Sheikh, and E. P. Simoncelli, “Image qualityassessment:from error visibility to structural similarity,” IEEE transac-tionsonimageprocessing,vol.13,no.4,pp.600–612,2004.
[19] Y. Wang, F. Liu, Z. Jiang, S. He, and Q. Mo, “Complex variational modedecomposition for signal processing applications,” Mechanical systems andsignalprocessing,vol.86,pp.75–85,2017.
[20] X.Wu,H.Hui,M.Niu,L.Li,L.Wang,B.He,X.Yang,L.Li,H.Li,
[21] J. Tian, et al., “Deep learning-based multi-view fusion model for screening2019 novel coronavirus pneumonia: a multicentre study,” European JournalofRadiology,vol.128,p.109041,2020.
[22] Y. Xia, B. Zhang, W. Pei, and D. P. Mandic, “Bidimensional multivari-ate empirical mode decomposition with applications in multi-scale imagefusion,”IEEEAccess,vol.7,pp.114261–114270,2019.
[23] X. Zhang, Y. Chen, R. Jia, and X. Lu, “Two-dimensional variational modedecomposition for seismic record denoising,”Journal of Geophysics andEngineering,vol.19,no.3,pp.433–444,2022.
[24] T.AlievaandA.M.Barb´e,“Self-fractionalfourierfunctionsandselection ofmodes,”JournalofPhysicsA:MathematicalandGeneral,vol.30,no.8,p.L211,1997.
[25] J. C. Nunes,Y. Bouaoune,E. Delechelle, O. Niang, and P. Bunel, “Im-age analysis by bidimensional empirical mode decomposition,” Image andvisioncomputing,vol.21,no.12,pp.1019–1026,2003.
[26] J.C.Nunes,S.Guyot,andE.Del´echelle,“Textureanalysisbased onlo- cal analysis of the bidimensional empirical mode decomposition,” MachineVisionandapplications,vol.16,pp.177–188,2005.
[27] Lee,J.Lee,J.Ko,J.Yoon,K.Ryu,andY.Nam,“Deeplearninginmr image processing,” Investigative Magnetic Resonance Imaging, vol. 23,no.2,pp.81–99,2019.
[28] S. Li, J. T. Kwok, and Y. Wang, “Combination of images with diversefocuses using the spatial frequency,” Information fusion,vol. 2, no. 3,pp.169–176,2001.
[29] G. Piella and H. Heijmans, “A new quality metric for image fusion,” inProceedings 2003 international conference on image processing (Cat. No.03CH37429),vol.3,pp.III–173,IEEE,2003.
[30] Y. Chen and R. S. Blum, “A new automated quality assessment algorithmfor image fusion,” Image and vision computing, vol. 27, no. 10, pp. 1421–1432,2009.
[31] H.ChenandP.K.Varshney,“Ahumanperceptioninspiredqualitymetricfor image fusion based on regional information,” Information fusion, vol. 8,no.2,pp.193–207,2007.
[32] Montalvo,C.Gavil´an,andA.Garc´ıa-Berrocal,“Variationalmodede- composition method (vmd) applied to decay ratio (dr) calculation for in-stabilities identification in bwr,” Nuclear Engineering and Design, vol. 390,p.111702,2022.
[33] M.F.Isham,M.S.Leong, M. H. Lim, and Z. A. Ahmad, “Variationalmode decomposition: mode determination method for rotating machinerydiagnosis,”Journal ofVibroengineering,vol.20,no.7,pp.2604–2621,2018.
[34] V. Tsagaris, “Objective evaluation of color image fusion methods,” OpticalEngineering,vol.48,no.6,pp.066201–066201,2009.
[35] Zosso,K.Dragomiretskiy,A.L.Bertozzi,andP.S.Weiss,“Two-dimensional compact variational mode decomposition:spatially compactand spectrally sparse image decomposition and segmentation,” Journal ofMathematicalImagingandVision,vol.58,pp.294–320,2017.
[36] Xiao, D. P. Bavirisetti, G. Liu, and X. Zhang, Image Fusion. Springer,2020.
[37] B.ShreyamshaKumar,“Multifocusandmultispectralimagefusionbasedon pixel significance using discrete cosine harmonic wavelet transform,”Signal,ImageandVideoProcessing,vol.7,pp.1125–1143,2013.
[38] V. Petrovic and C. Xydeas, “Objective image fusion performance charac-terisation,” in Tenth IEEE International Conference on Computer Vision(ICCV’05)Volume1,vol.2,pp.1866–1871,IEEE,2005.